Optimization of Piecewise-Focusing CST collectors using the System Advisor Model, and comparison to a central receiver system

David K Bisset

Research Engineer

Canberra ACT Australia

Email: davidkbisset@gmail.com

ABSTRACT

Heat collection performance simulations using the System Advisor Model (SAM) with Typical Meteorological Year weather data from four geographic locations are used to investigate (a) the optimum overall tilt of Piecewise-Focusing (PWF) collectors, and (b) PWF collector performance in comparison to the SAM default central receiver system. Results show that the overall tilt angle is not critical, but values up to 50 degrees are best at non-tropical latitudes, even when output in summer is more valuable than in winter. For tropical latitudes, 40 degrees of tilt is sufficient. Increasing PWF collector width relative to height is advantageous. Depending on location, PWF collector performance is 66% to 90% better than for the SAM default 100 MW_e central receiver system, per m^2 of reflector or heliostat. Using SAM's detailed control over system parameters, it

is shown that the PWF collector's superior performance is derived mainly from better geometry (smaller cosine losses), but the near-absence of atmospheric attenuation and the smaller receiver heat losses are also significant.

1 INTRODUCTION

The System Advisor Model (SAM) simulation software [1] from the USA National Renewable Energy Laboratory is widely used for investigating concepts and designing projects for many types of renewable energy generation, including Concentrating Solar Thermal (CST) systems. Simulations of CST operation may be carried out on an hour-by-hour basis for an entire year, based on realistic weather data such as Typical Meteorological Year (TMY) files for specific locations of interest. Two features of SAM are utilized for the present work. Firstly, SAM includes a detailed physics-based model of a 100 MW_e central receiver ('power tower') system. Secondly, SAM has a 'generic' CST facility, in which the performance of any type of CST collector is modelled by a table of optical efficiencies as a function of solar azimuth and zenith angles. The two systems incorporate very similar molten salt thermal storages and steam-turbine power blocks, and therefore realistic comparisons of system performance on the same weather data may be carried out. However, parasitic power losses are significant for the central receiver system, e.g. heat transfer fluid (HTF) pumping power is 3-4% of gross turbine output, and equivalent losses are undetermined for Piecewise-Focusing (PWF) systems [2]. Therefore the best aspect for comparison between systems is the amount of heat in the HTF as it leaves the receiver(s), per m^2 of heliostat or reflector. This is also the relevant output for industrial process heat applications.

The PWF collector was described and analyzed in the paper by Bisset [2], and the need for optimization in certain aspects of design (especially overall collector tilt) was noted. Also the comparison with central receiver systems was based on general estimates rather than realistic weather-based simulations. The present

paper takes up these issues using SAM in the context of TMY data at four locations with different latitudes and climates. Then the performance comparisons between PWF collectors and central receiver systems are broken down into various stages as sunlight is collected, concentrated, and converted into usable heat, since SAM allows detailed control of settings for efficiencies and losses. Finally, both types of CST system are briefly compared to photovoltaic panel systems with battery storage.

2 SAM CONFIGURATION

2.1 Weather data

The four sets of TMY weather data used in the simulations are listed in Table 1. All come from the USA National Solar Radiation Database (NSRDB) [3]; the first two are supplied by default with the SAM distribution, and the others were downloaded directly. Daggett and Des Moines, being quite some distance from the equator, exhibit considerable variation between summer and winter solar direct normal insolation (DNI). Daggett has a near-desert climate with a big majority of clear days, while Des Moines has more

Table 1. TMY weather data from the NSRDB [3]

Location	Lat & Long, deg	Annual DNI, kWh/m^2	NSRDB station ID
Daggett, California	34.9, −116.8	2799	91486 (via SAM)
Des Moines, Iowa	41.6, −93.6	1591	757516 (via SAM)
North-central Mexico	23.3, −102.5	2789	549592
Northern Chile	−21.0, −69.2	3387	1399660

cloudy days overall, and has the shortest daylight hours in winter. The Mexico data come from a semi-desert region with clear winter days and rain falling mainly around late summer; the annual DNI is virtually the same as at Daggett but the seasonal pattern is quite different. The solar resource for the Atacama Desert of northern Chile is among the highest to be found anywhere, with high values of DNI throughout the year.

2.2 The SAM central receiver system

The default 100MW_e central receiver system, with 10 hours of thermal storage and a solar multiple (which determines heliostat total area) of 2.4, is somewhat over-specified for operations in summer (although this improves electricity output during other seasons). The result is that a significant fraction of the heliostat field must be defocused on clear summer days when the thermal storage reaches full capacity. Since the point of comparison in this paper concerns the maximum heat collected per square metre of heliostat (or reflector), the default settings were adjusted until defocusing no longer occurred — 16 hours of thermal storage (18 hours for Chile) and solar multiple 2.3. The layout of this slightly reduced heliostat field was re-optimized without changing tower or receiver dimensions.

2.3 The Piecewise-Focusing collector

Approximately 250 independent reflectors are mounted on a base-frame, collectively forming a roughly paraboloidal surface with its focus at the entrance to a cavity receiver. The entire collector rotates about a vertical axis in order to follow the azimuthal position of the sun, while the reflectors rotate about nearly horizontal axes (which are at different particular angles to the base-frame) to track the sun's elevation above the horizon. Details of the design calculations are given in [2], and a simplified 3D model is shown in Fig.1. The axis of the paraboloidal surface (passing through the cavity receiver) is tilted towards the sun by a fixed angle (30 degrees for the model in Fig. 1) that is appropriate for any given geographical location, investigated in Section 4. This overall angle of tilt (among other factors) influences the values in the table

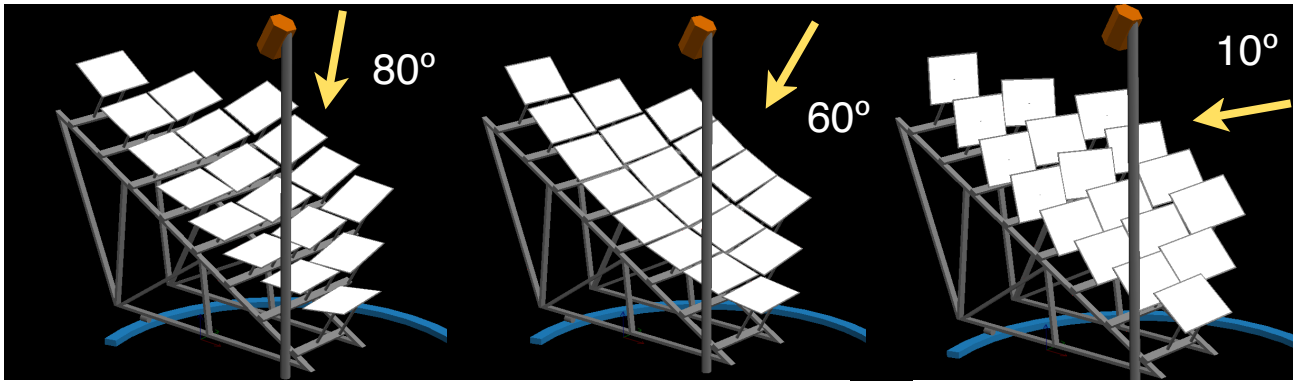

Fig. 1. Simplified 3D model of a paraboloidal PWF collector using oversize reflectors, sourced from [2]. For clarity, only the right-hand half is shown. Reflectors are tilted around their mounting axes as required for the three indicated sun elevations.

of optical efficiencies that SAM uses for 'generic' CST simulations. Values for any given sun elevation angle are the same in the table for all 360 degrees of azimuth, as required by the PWF collector's azimuthal rotation to keep facing the sun. The methods of calculating table values are described in Section 4. SAM solar field default values are used except for the following settings: deploy/stow angles 0/180 degrees; cleanliness factor 0.97; general optical derate 0.92; reference thermal loss fraction 0.052; and irradiation thermal loss adjustment parameters 0.9, -0.7, 0.6, 0.0. All other loss adjustment parameters are zeroed. With these settings, receiver thermal losses match those estimated in [2].

Default settings of the 100 MW_e steam turbine power block (the destination of collected heat either directly or via storage) were retained. Thermal storage in SAM was set at 16 hours (as for the central receiver), but the solar multiple was reduced to 2.0 or less (depending on location) because of the PWF collector's greater efficiency, to avoid any dumping of excess heat. Note that although SAM provides an estimate of reflector area required to achieve the specified output, the actual area to be used for each set of conditions is recalculated at the beginning of the simulation run and must be checked in the results. In practice a number of PWF collectors connected to the central power block will be required to make up this

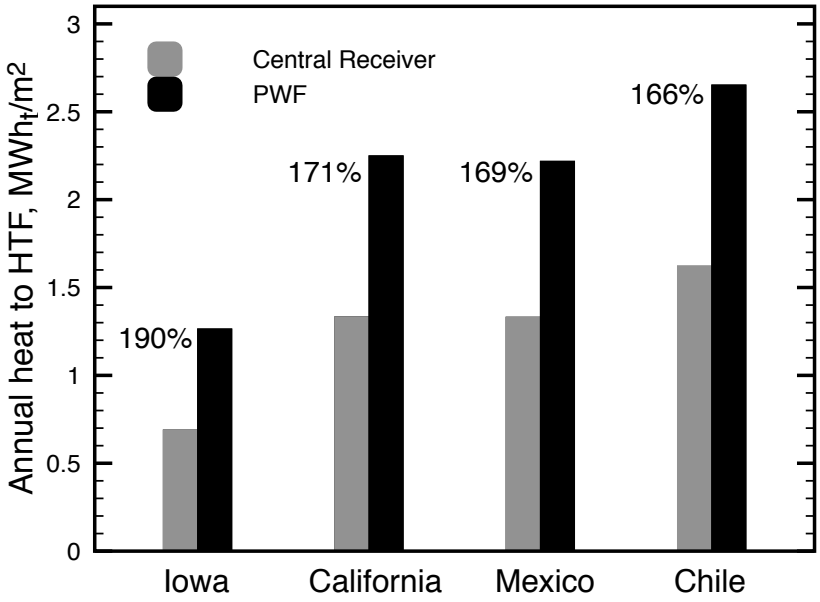

Fig. 2. Annual heat collected in the HTF per m^2 of reflector (PWF) or heliostat (central receiver) at four locations.

total area (because of practical limits to their size), but this has no effect on SAM results.

3 COMPARISON OF HEAT COLLECTION PERFORMANCE

Results for heat energy collected in the HTF per year, per m^2 of heliostat or reflector, are shown in Figure 2, where the PWF data come from the optimizations described in the following section. Heat output increases with annual DNI as expected, but the PWF output is always greater than that of the central receiver by factors shown as percentages on the figure. The previous general estimate [2], that equal heat output can be obtained from an area of PWF reflectors that is 62% of central receiver heliostat area, corresponds to 161% heat output per m^2. The reasons for the far higher production from PWF collectors are examined in Section 6. These results suggest that PWF power plants are likely to be smaller and cheaper than central receiver systems of equal output, and they may also be economically feasible in regions of moderate DNI, closer to load centres, where central receiver systems are uneconomical.

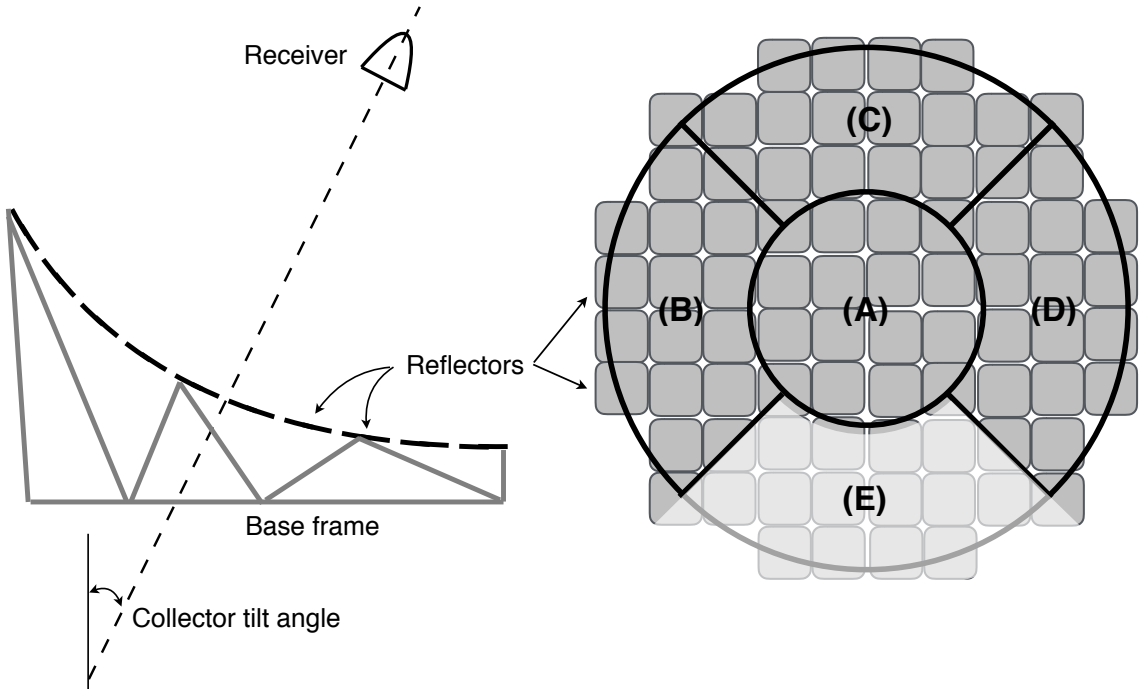

Fig. 3. Cross-section side view of PWF collector (left), and view into the aperture from the receiver (right). Sectors A-E are of equal area, and sector E is removed for shape optimization. The side view (left) corresponds to 60 degrees of sun elevation in Fig. 1.

4 OPTIMIZATION OF PWF COLLECTOR TILT AND SHAPE

Ideally, the 250 or so reflectors in a PWF collector broadly follow a paraboloidal surface, the axis of which is tilted towards the sun. However, unlike the paraboloidal dish upon which it is loosely modelled, the PWF collector's overall angle of tilt is fixed (Figure 3, left). This permits much more economical construction and larger sizes than for a dish, while retaining much of the dish's high optical efficiency. The optimum tilt is expected to be different for locations at different latitudes. Initially the overall collector aperture (Figure 3, right) is assumed to be circular. As can be seen in Figure 3 (left), individual reflectors lean in towards the collector axis by up to 22.5 degrees; a suitable weighted average value is 16 degrees. Therefore, entries for the SAM table of optical efficiencies were calculated as cos16[cos(zenith−tilt)], where zenith = 90−elevation. (SAM mainly uses azimuth/zenith angles for sun position rather than azimuth/elevation.)

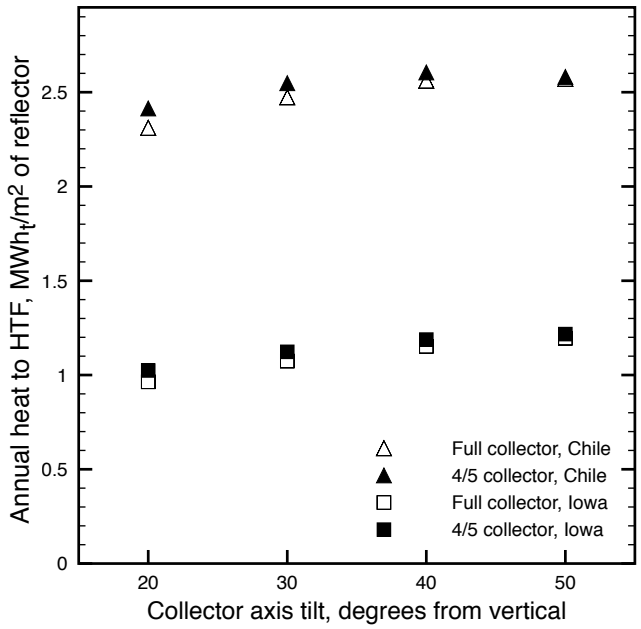

Fig. 4. Annual heat collection as a function of overall collector axis tilt for locations at low (Chile) and high (Iowa) latitude. See text for explanations of full and 4/5 collectors. Simulation parameters as given in Section 2.3.

Simulations were run for all weather locations at overall tilt angles of 20, 30, 40, and 50 degrees. Heat collection results for Iowa and Chile, labelled 'full collector', are given in Figure 4.

Although the amount of heat collected is not a strong function of overall tilt, it is clear that larger tilt values are better — at least 40 degrees for low latitudes such as the Chile location, and 50 degrees for higher latitudes. For a circular aperture, increasing tilt rapidly increases the height of the collector's upper rim from the ground, resulting in greater wind loading as well as greater cost of construction. One way of counteracting this issue is to remove some of the reflectors at the lower part of the rim, so that the overall collector shape is wider relative to its height, and the majority of reflectors and the receiver are closer to ground level. Also, reflectors in the lower part have the greatest potential for astigmatism (and thus spillage) when the sun elevation is low [2]. Reflector removal was accomplished for modelling purposes by dividing the collector aperture into five equal sectors, labelled A to E in Figure 3 (right), and deleting the lowest

Table 2. Calculation of SAM optical efficiency by sector. Angles are in degrees.

Sector	Optical efficiency
A	cos(zenith−tilt)
B,D	cos17[cos(zenith−tilt)]
C	cos(zenith−tilt−17)

one, sector E. Entries for the SAM table of optical efficiencies were calculated as the average of efficiencies for sectors A-D (Table 2), noting that sectors B-E lean in towards the collector axis by 17 degrees. Heat collection results for this modified collector, termed '4/5 collector', are compared with the full collector results in Figure 4. Improvements in heat collection using the 4/5 collector are only modest, but they are very worthwhile when the benefits in terms of collector construction are taken into account.

5 VARIATIONS IN SEASONAL AND HOURLY PERFORMANCE

Only the annual total of heat collected has been considered so far, but the variation from month to month can be quite significant (depending on geographical location), and the passage of the sun across the sky is the primary factor in real-time output. In regions with mild winters and hot summers the value of electricity may be highest by far on summer evenings, and therefore a PWF collector could be designed for best performance in summer, with weaker winter performance as a trade-off. In cooler climates the reverse might apply. Seasonal variations for different collector tilts and shapes are examined in Figure 5 using Mexico (latitude 23.3 degrees) and Iowa (latitude 41.6 degrees) weather data. At noon in the summer

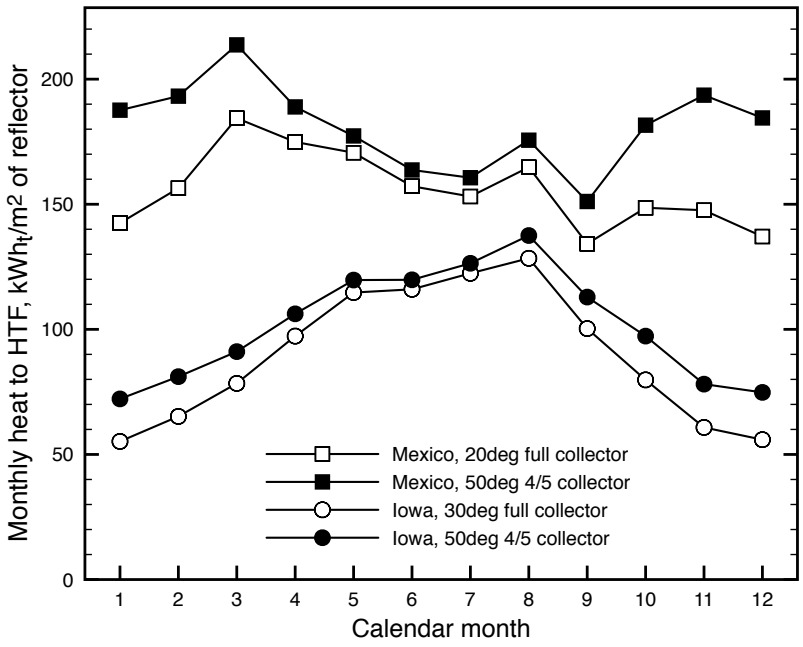

Fig. 5. Monthly heat output for different collector tilt angles for two sets of weather data. Higher tilt improves winter output without any loss of output in summer. SAM simulation parameters are as given in Section 2.3.

months (June, July, August) the solar zenith angle in SAM for the Mexico location ranges from 5 to 16 degrees, suggesting that 20 degrees of collector tilt could be appropriate for best results in summer. For Iowa, the equivalent noon zenith angles are 18 to 33 degrees, and 30 degrees of tilt seemed appropriate. Results for the 4/5 collector tilted at 50 degrees, emphasizing winter output, are also shown.

As expected, the output curves from the less-tilted collectors (Figure 5) show sharper decreases from summer to winter compared to the curve from the 50-degree-tilted collector (the effects of a dry winter and late summer rainfall can also be seen in the Mexico results, but the implications for collector tilt are unchanged). However, the highly-tilted collector gives higher output for every month, even in summer (marginally). The opportunity to simulate performance from realistic weather data in SAM leads to the somewhat surprising conclusion that a highly-tilted collector works better all year round in a wide range of locations.

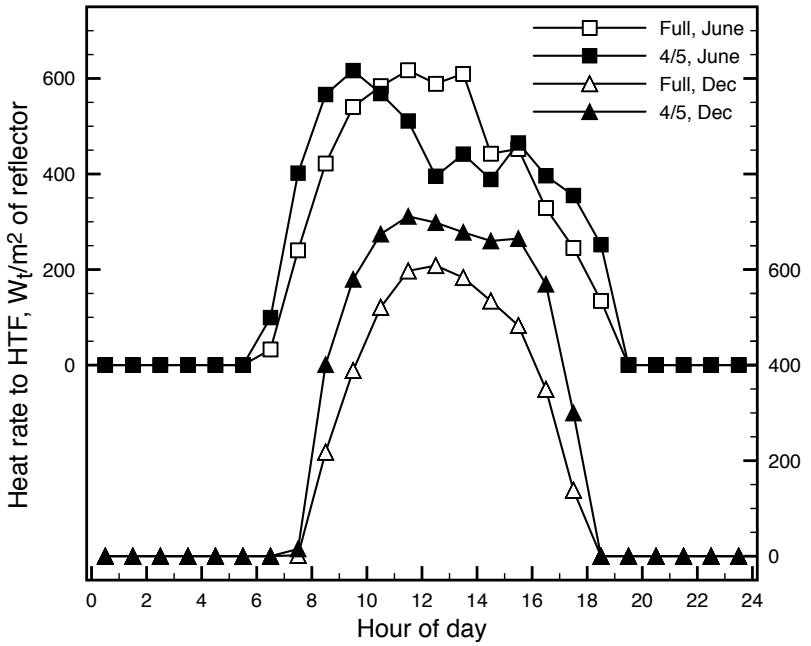

Fig. 6. Summer (June) and winter (December) heat output over the course of a day for two collector designs: full collector tilted 20 degrees, and 4/5 collector tilted 50 degrees. Hourly heat rates are averages for the given month, extracted from the Mexico SAM simulations used for Fig. 5.

The reason for the 50-degree-tilted collector's good performance in summer (as well as in winter) was explored in hour-by-hour profiles for June in the Mexico data (Figure 6), with December (winter) results also shown. The PWF collector's optical efficiency is highest when the sun's zenith angle is more-or-less aligned with collector tilt, which is the case for the full collector (20 degree tilt) for four hours or so around noon in summer. The 4/5 collector (50 degree tilt) is not as well aligned at these times, and output is substantially lower. However, it is better aligned than the full collector for several hours after sunrise and several hours before sunset, and the greater output at these times compensates for lower output in the middle of the day. In December, where the sun zenith angle is not less than 45 degrees for this location, the more tilted 4/5 collector has a significant advantage throughout the day (Figure 6).

6 CAUSES OF INEFFICIENCY AND HEAT LOSS

The ideal maximum rate of heat collection for any CST collector is the product of total reflector area and DNI, and as shown in Figure 2, PWF collectors approach the maximum per m^2 (the annual DNI from Table 1) much more closely than central receiver systems. SAM simulations include the effects of many factors that influence the actual rate of heat collection in the HTF. The procedure in this section was to switch off all possible losses and inefficiencies, and then repeat the simulations with the losses/inefficiencies restored step-by-step, as much as possible in the order from incoming sunlight, reflector, receiver, to HTF. The step-by-step decrease in heat collected represents the effect of each loss or inefficiency. It was confirmed that "Field Incident Thermal Power" in the first step of the central receiver simulation (with heliostat stow/deploy angle reduced from 8 degrees to 1 degree) was very close to the ideal maximum, and equivalent checks were made for the SAM generic CST simulation (i.e. the PWF results). Storage and power block parameters were adjusted as necessary to absorb the additional heat reaching the HTF, avoiding heliostat defocusing and excess heat dumping.

Figure 7 shows the inefficiencies and losses that reduce actual heat collected relative to the potential maximum. The SAM default central receiver system uses a heliostat field that fully surrounds the central receiver tower, which means that most heliostats are at quite oblique angles to the sun for much of the time, and therefore cosine losses are very significant. Shading and blocking of nearby heliostats when the sun is at a low angle are minor problems, included within the 'geometry' loss in Figure 7. Reflectors of the PWF collector are always much more 'square-on' to the sun with correspondingly lower cosine losses, and there is no mutual blocking, only some shading when the sun is off-axis. The central receiver geometry loss is almost four times as large as that of the PWF.

Mirror reflectivity and soiling, reflector/heliostat availability and receiver/tower shadow are similar for the two systems, as is spillage caused by slope errors of mirror surfaces.

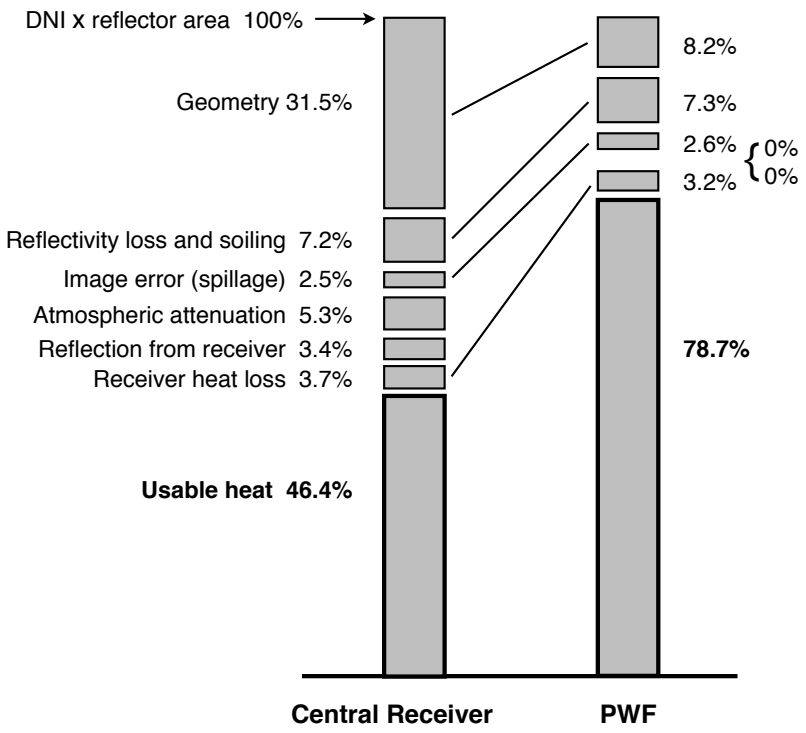

Fig. 7. Disposition of actual and potential heat collection using the California (Daggett) TMY weather data.

Atmospheric attenuation is negligible for the relatively compact PWF collectors, but can be quite serious for a central receiver system where the outermost heliostats are nearly 2 km from the receiver. The default values of the polynomial in slant range that SAM uses for attenuation result in the 5.3% loss shown (this is 8.8% of the sunlight impinging on the receiver). Inferring from the study by Polo, Ballestrin and Carra [4], the defaults apply for a reasonably clean atmosphere with occasional moderate levels of smog or dust, or equivalent. Large central receiver systems will be badly affected at locations with significant sources of scattering or absorption in the atmosphere.

By default, absorptivity of the central receiver surface is 94%, i.e. 6% of impinging sunlight is reflected, which is 3.4% of maximum sunlight. Absorption of the PWF cavity receivers is assumed 100%. Heat loss from receivers by convection and re-radiation is fairly similar for the two systems as a percentage of maximum sunlight, with PWF loss parameters set to match the receiver loss estimated in [2]. The final result

is that less than half the available sunlight heat energy is absorbed by the HTF in the central receiver system, while more than three-quarters of it reaches the HTF in the PWF system.

Summarising, PWF collectors perform better than the central receiver system because the latter loses 3.9 percentage points more heat at the receiver, 5.3 percentage points from atmospheric attenuation, and 23.3 more percentage points through inferior geometry (mainly cosine losses).

7 DISCUSSION

The simulations carried out with SAM using TMY weather data from four locations have shown that PWF collector systems collect 66% to 90% more heat than central receiver systems, per m^2 of reflector/heliostat, and have explained why this is so. PWF collector systems (as currently proposed) use the same molten salt heat storages and steam-Rankine power blocks as central receiver systems, so the electricity output will be greater by very similar proportions.

7.1 PWF collector design

The overall shape of PWF collectors can be varied over quite a wide range of possible designs, and there may be trade-offs between performance and construction cost, but results so far suggest that the collector overall axis should be tilted away from vertical by 40 or 50 degrees, and that overall width should be greater than height. The mounting axis angles [2] for each reflector depend only on its position relative to the receiver, which means that the overall surface shape formed by the combined reflectors does not need to be paraboloidal; for example it could be a flat surface tilted appropriately. Small gaps between adjacent reflectors would be needed to reduce shading and blocking losses. The paraboloidal shape is convenient for use in SAM because the optical efficiency values can be found analytically (Fig. 3 and Table 2).

The sun-elevation tracker for each reflector can be an off-the-shelf linear actuator, much cheaper than heliostat drives. The overall length, width, and height for a PWF base-frame will be quite large (of order 50

to 100 m), but there are no large concentrated forces anywhere since wind and gravity loads from the many reflectors are widely distributed. Most likely lattice-truss or space-frame construction will be used, quite like that of typical high-voltage electricity pylons, which are very light for their size and strength. Adverse weather conditions must be allowed for in the design. The broad footprint of the base-frame helps in coping with high wind forces, and the reflectors should be capable of being set horizontally to minimize extreme wind forces. Also it should be possible to angle the reflectors away from the direction of hail during severe hailstorms.

7.2 Comparison to photovoltaic panels with battery storage

How do CST systems with thermal storage compare to PV systems with lithium ion battery storage? PV-battery systems are undoubtedly more economical for small applications and short storage periods (less than 50 MW, less than 3 hours or so of full-power output from batteries), and CST is more competitive at larger scale (e.g. 110 MW and 17.5 hours storage for the Cerro Dominador central receiver system [5]). However many different battery chemistries are now being investigated [6], some of which are directly aiming to reduce the cost of large stationary batteries. As the cost of batteries declines, the long-term economic viability of larger CST systems will be questioned, even when 'Gen 3' versions [7] of CST are available in future.

The following comparison is based on electricity output per unit area of active surface (mirrors or PV panels), which is somewhat artificial given the very different technologies involved, but it does indicate the relative sizes of different systems that have to be balanced against different costs per unit area. SAM includes a detailed PV system model that allows a wide choice of PV panels and inverters with measured performance data, and offers the 1-axis tracking system that is typically used by modern utility-scale PV installations. The same California (Daggett) TMY weather file is used here, but PV panels respond to diffuse

Table 3. Annual electricity output per m^2 of PV panel or mirror, for California (Daggett)

System type	Annual output, kWh_e/m^2
PV panels and lithium-ion battery	492
Heliostats and central receiver, molten salt, steam turbine	471
PWF collectors, molten salt, steam turbine	807

insolation as well as DNI, which increases output by about 12%. With selected high-efficiency PV modules (21.9%) and inverter the annual electricity output is 559 kWh/m^2. After storage in lithium-ion batteries with a round-trip efficiency of 88% (a representative figure from measurements [8]), the final annual output is 492 kWh/m^2. The SAM central receiver thermal storage efficiency on a 24-hr cycle is about 99%, and power block efficiency is about 37% after allowing for parasitics; the California thermal results (Figure 2) were multiplied by these efficiencies and are shown in Table 3 along with the PV result.

In spite of the CST power block's considerably higher efficiency than that of the PV modules, the electricity generation per m^2 of heliostat is slightly less than generation per m^2 of PV panel. Central receiver systems will have to cost *less* per m^2 than PV-battery systems, quite difficult to achieve unless storage is required for many hours, e.g. [5]. Generation from a PWF collector system is much higher, and although the cost of construction has not been determined, the PWF system will have the certain advantage of being a lot smaller than either PV-batteries or a central receiver system for the same output.

7.3 CST process heat

Industrial process heat applications at 200 C to 500 C could use the heat stored in molten salt directly, avoiding the inherent thermodynamic losses in converting heat to electricity. For example, a report commissioned by the Australian Renewable Energy Agency [9] shows that the largest industrial use of heat in Australia is for the production of alumina from bauxite, and about two-thirds of that heat is required for producing steam at 200 C to drive the digestion stage of the Bayer process [9]. The digestion of nickel-cobalt ore at 255 C is another big use of heat [10]. PWF systems have the advantage of far higher efficiency in regions of moderate DNI (Figure 2) where such applications are more likely to be found.

REFERENCES

[1] System Advisor Model Version 2020.11.29 rev 2, National Renewable Energy Laboratory, Golden, CO.

[2] Bisset, D.K., 2022, "Piecewise-Focusing Collectors Reduce the Mirror Area in Concentrating Solar Thermal Power Plants", ASME J. Sol. Energy Eng., **144**(5) p. 055001. doi: https://doi.org/10.1115/1.4054027

[3] National Solar Radiation Database, 2021, National Renewable Energy Laboratory, Golden CO.

[4] Polo, J., Ballestrin, J., Carra, E., 2016, "Sensitivity study for modelling atmospheric attenuation of solar radiation with radiative transfer models and the impact in solar tower plant production", Solar Energy **134** pp. 219–227. http://dx.doi.org/10.1016/j.solener.2016.04.050

[5] Institute for Advanced Sustainability Studies, 2021, "Atacama I / Cerro Dominador 110MW CSP + 100 MW PV CSP Project", National Renewable Energy Laboratory, Golden, CO.

[6] Passerini, S. and Li, J. (eds), 2021, "Focus Review — New and Emerging Battery Technologies", J. Power Sources **484**, article 229333. doi: 10.1016/j.jpowsour.2020.229333

[7] Mehos, M., Turchi, C., Vidal, J., Wagner, M., Ma, Z., Ho, C., Kolb, W., Andraka, C., and Kruizenga, A., 2017, *Concentrating Solar Power Gen3 Demonstration Roadmap,* National Renewable Energy Laboratory, Golden, CO, Report No. NREL/TP-5500-67464.

[8] Battery Test Centre, 2022, *Public Report 12 (Final Report),* ITP Renewables, Turner ACT Australia.

[9] Lovegrove, K., Alexander, D., Bader, R., Edwards, S., Lord, M., Mojiri, A., Rutovitz, J., Saddler, H., Stanley, C., Urkalan, K., and Watt, M., 2019, *Renewable Energy Options for Industrial Process Heat,* ITP Thermal Pty Ltd, Turner ACT Australia.

[10] Beath, A., Meybodi, M. and Drewer, G., 2022, "Techno-economic assessment of application of particle-based concentrated solar thermal systems in Australian industry", J. Renewable Sustainable Energy **14**, 033702. doi: 10.1063/5.0086655

8 TABLE CAPTIONS

1. TMY weather data from the NSRDB [3]

2. Calculation of SAM optical efficiency by sector. Angles are in degrees.

3. Annual electricity output, kWh/m^2 of PV panel or mirror, for California (Daggett)

9 FIGURE CAPTIONS

1. Simplified 3D model of a paraboloidal PWF collector using oversize reflectors, sourced from [2]. For clarity, only the right-hand half is shown. Reflectors are tilted around their mounting axes as required for the three indicated sun elevations.

2. Annual heat collected in the HTF per m^2 of reflector (PWF) or heliostat (central receiver) at four locations.

3. Cross-section side view of PWF collector (left), and view into the aperture from the receiver (right).

Sectors A-E are of equal area, and sector E is removed for shape optimization. The side view (left) corresponds to 60 degrees of sun elevation in Fig. 1.

4. Annual heat collection as a function of overall collector axis tilt for locations at low (Chile) and high (Iowa) latitude. See text for explanations of full and 4/5 collectors. Simulation parameters as given in Section 2.3.

5. Monthly heat output for different collector tilt angles for two sets of weather data. Higher tilt improves winter output without any loss of output in summer. SAM simulation parameters are as given in Section 2.3.

6. Summer (June) and winter (December) heat output over the course of a day for two collector designs: full collector tilted 20 degrees, and 4/5 collector tilted 50 degrees. Hourly heat rates are averages for the given month, extracted from the Mexico SAM simulations used for Fig. 5.

7. Disposition of actual and potential heat collection using the California (Daggett) TMY weather data.